XVIII IMEKO WORLD CONGRESS
Metrology for a Sustainable Development
September, 17 – 22, 2006, Rio de Janeiro, Brazil

GLOBAL-OPTIMIZATION APPROACH OF SPECTRUM RECONSTRUCTION

Andrzej Miękina[1], *Roman Z. Morawski*[2]

[1]Warsaw University of Technology, FE&IT, Institute of Radioelectronics, Warsaw, Poland, e-mail: a.miekna@ire.pw.edu.pl
[2]Warsaw University of Technology, FE&IT, Institute of Radioelectronics, Warsaw, Poland, e-mail: r.morawski@ire.pw.edu.pl

Abstract: The paper is on the usefulness of global optimization for developing variational algorithms of spectrophotometer calibration. A new nonlinear method for reconstruction of absorption spectrum, on the basis of spectrophotometric data, is proposed and used for demonstrating that the quality of reconstruction depends on the ability of the calibration procedure to reach a global minimum during optimization of the parameters of the operator of reconstruction. The results obtained using calibration algorithms based on local and global optimization are compared in terms of measurement uncertainty and artefact content.

Keywords: optical spectroscopy, spectrophotometric data processing, spectrum estimation, global optimization

Notation:

λ	–	wavelength $\lambda \in [\lambda_{\min}, \lambda_{\max}]$;
N	–	the number of spectral data in one set;
$\Delta\lambda$	–	the average wavelength step $\Delta\lambda = \frac{\lambda_{\max} - \lambda_{\min}}{N-1}$;
λ_n	–	$\lambda_n = \lambda_{MIN} + (n-1)\Delta\lambda$ for $n = 1, .., N$;
$x(\lambda)$	–	the spectrum;
$\mathbf{x}$	–	the vector of spectrum samples;
$\hat{\mathbf{x}}$	–	an estimate of the vector $\mathbf{x}$;
$\tilde{\mathbf{y}}$.	–	the spectrophotometric data;
$\boldsymbol{\eta}$	–	the vector of noise corrupting the data $\tilde{\mathbf{y}}$;
$\circ\mathscr{M}$	–	an operator for modeling the data;
$\mathbf{p}_{\circ\mathscr{M}}$	–	the vector of the parameters of the operator $\circ\mathscr{M}$;
$\mathscr{R}$	–	an operator for spectrum reconstruction;
$\mathbf{p}_{\mathscr{R}}$	–	the vector of the parameters of the operator $\mathscr{R}$.

1. INTRODUCTION

The computer-based interpretation of spectrometric data $\tilde{\mathbf{y}} = [\tilde{y}_1, ..., \tilde{y}_N]^T$, aimed at identification of the chemical composition of an analyte, is of great importance for applications of various kinds of spectroscopy in science, biomedical engineering, environmental engineering and industry – *cf.* [1]-[13]. The first step of interpretation usually consists in estimation of the absorbance spectrum of the analyte $x(\lambda)$; many methods for solving that problem have been developed, for example [14]-[25]. The older methods, whose examples may be found in [14], are based on a forward model of the data, being a linear or weakly nonlinear integral operator:

$$x(\lambda) \rightarrow \tilde{\mathbf{y}} \tag{1}$$

which after discretisation takes on the form:

$$\tilde{\mathbf{y}} = \circ\mathscr{M}[\mathbf{x}; \mathbf{p}_{\circ\mathscr{M}}] + \boldsymbol{\eta} \tag{2}$$

where $\mathbf{x} = [x_1, ..., x_N]^T$, $x_n = x(\lambda_n)$, $\circ\mathscr{M}$ is a linear or weakly nonlinear algebraic operator whose parameters $\mathbf{p}_{\circ\mathscr{M}}$ are to be determined during calibration of the spectrometer, and $\boldsymbol{\eta}$ is a vector modelling random noise in the data. In this case, the spectrum estimation consists in (pseudo)inversion of the operator $\circ\mathscr{M}$ for each vector of the data $\tilde{\mathbf{y}}$. The more modern methods, whose examples may be found in [21] and [24], are based on the inverse model of the data, being a nonlinear algebraic operator of generalized deconvolution:

$$\hat{\mathbf{x}} = \mathscr{R}[\tilde{\mathbf{y}}; \mathbf{p}_{\mathscr{R}}] \tag{3}$$

whose parameters $\mathbf{p}_{\mathscr{R}}$ are to be determined during calibration of the spectrometer. In this case, the spectrum estimation consists in direct application of the operator $\mathscr{R}$ to the data $\tilde{\mathbf{y}}$.

The above-outlined approaches differ in several important features: the attainable accuracy and numerical complexity of spectrum estimation, the numerical complexity of calibration, and the requirements concerning the data for calibration.

According to the inverse-model-based approach, the operator $\mathscr{R}$ may be globally optimized using the criteria of the quality of spectrum estimation (defined in the space of spectra). The attainable accuracy of spectrum estimation is higher for this approach than for the forward-model-based approach since the latter is based on the optimization of the operator $\circ\mathscr{M}$ using the criteria of the quality of measurement channel simulation, defined in the space of vectors of data.

If the use of a linear and stationary forward model of the measurement channel is sufficient, then the numerical complexity of its identification, performed during calibration, is – as a rule – much lower than that of the identification of the corresponding operator $\mathscr{R}$ that must be nonlinear to warrant the stability of the solution. It increases quickly, however, when a non-stationary model has to be used, and becomes comparable if non-linearity must be introduced. The same reasoning applies to the requirements

concerning the data for calibration.

According to the forward-model-based approach, the operator $\mathscr{R}$ is created during the process of spectrum estimation by referring to the forward model of the measurement channel $\mathscr{M}$. Consequently, the numerical complexity of the algorithms of spectrum reconstruction based on this approach is – as a rule – significantly higher than that of the comparable algorithms based on the inverse-model-based approach.

2. RESEARCH OBJECTIVE

This paper is devoted to a new operator $\mathscr{R}$ and methods of its identification using tools of global optimization. It is defined by the formula:

$$\hat{x}_n = F_2\left[\sum_{\nu=-3}^{3} b_\nu F_1\left(\tilde{y}_{n-\nu}\right)\right] \text{ for } n = 4, ..., N-3 \tag{4}$$

where $F_1(z)$ and $F_2(z)$ are functions in one variable defined as follows:

$$F_1(z) = z^3 + a_2 z^2 + a_1 z + a_0 \tag{5}$$

$$F_2(z) = \frac{1}{\pi}\arctan(z) + \frac{1}{2} \tag{6}$$

Thus, the vector of the parameter of the operator $\mathscr{R}$ contains 10 elements, *viz.*:

$$\mathbf{p}_{\mathscr{R}} = [a_0\ a_1\ a_2\ b_{-3}\ b_{-2}\ b_{-1}\ b_0\ b_1\ b_2\ b_3]^T \tag{7}$$

They are to be estimated during calibration via minimization of the following criterion:

$$J[\mathbf{p}_{\mathscr{R}}] = 0.75\left\|\mathscr{R}\left[\tilde{\mathbf{y}}^{cal}; \mathbf{p}_{\mathscr{R}}\right] - \mathbf{x}^{cal}\right\|_2 + 0.25\left\|\mathscr{D}\circ\mathscr{R}\left[\tilde{\mathbf{y}}^{cal}; \mathbf{p}_{\mathscr{R}}\right]\right\|_2 \tag{8}$$

where $\mathbf{x}^{cal}$ and $\tilde{\mathbf{y}}^{cal}$ are reference data used for calibration, and $\mathscr{D}$ is the operator of numerical differentiation.

For the sake of numerical simplicity, the optimization problems of this type are, as a rule, solved by means of the methods of local rather than global optimization. The research to be reported in the paper is aimed at studying the consequences of this simplification for the measurement uncertainty.

3. RESEARCH METHODOLOGY

The method of spectrum reconstruction, defined in the previous section, has been systematically studied using synthetic data whose noise-free version is shown in Fig. 1 ($\dot{\mathbf{x}}^{cal}$ and $\dot{\mathbf{y}}^{cal}$ used for calibration) and Fig. 2 ($\dot{\mathbf{x}}^{val}$ and $\dot{\mathbf{y}}^{val}$ used for validation). All experiments have been first performed for the noise free-data and then repeated for the data corrupted with additive noise:

$$\tilde{y}_n^{cal} = \dot{y}_n^{cal} + \eta_n^{cal} \text{ for } n = 1, ..., N \tag{9}$$

$$\tilde{y}_n^{val} = \dot{y}_n^{val} + \eta_n^{val} \text{ for } n = 1, ..., N \tag{10}$$

where η_n^{cal} and η_n^{val} are zero-mean, uniformly distributed, pseudo-random numbers with a known standard deviation $\sigma_\eta \in \{10^{-4}, 10^{-3}\}$; $N = 200$.

All experiments have been carried out in two ways: by using a MATLAB procedure of local optimization *fminunc* and a TOMLAB procedure of global optimization *glbSolve*. The results have been compared using the following indicators of the uncertainty of spectrum reconstruction:

$$\Delta_2[\hat{\mathbf{x}}] = \frac{1}{\sqrt{N}}\left\|\hat{\mathbf{x}} - \dot{\mathbf{x}}\right\|_2 \text{ and } \Delta_\infty[\hat{\mathbf{x}}] = \left\|\hat{\mathbf{x}} - \dot{\mathbf{x}}\right\|_\infty \tag{11}$$

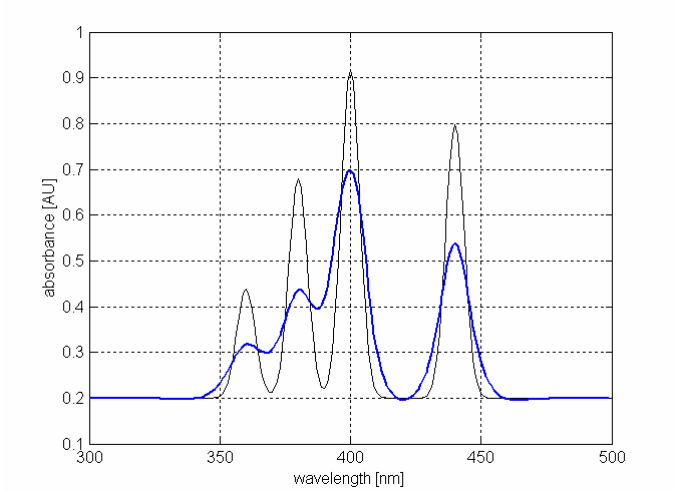

Fig. 1. The spectrum (thin line) and the data (bolder lighter line) used for calibration.

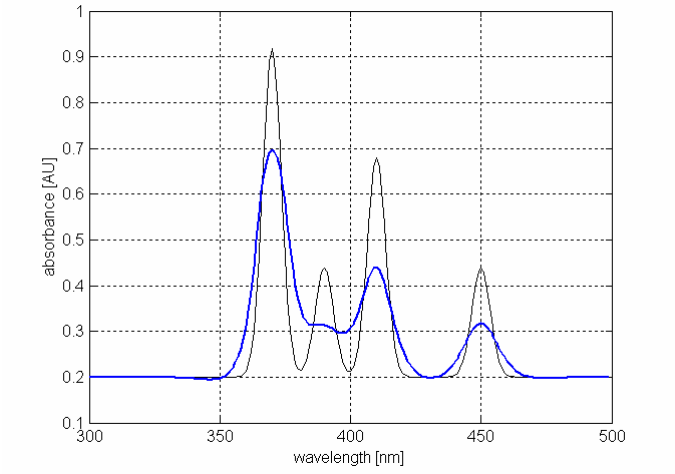

Fig. 2. The spectrum (thin line) and the data (bolder lighter line) used for validation.

3. RESULTS OF STUDY

The numerical results of the study are summarized in Table 1. The difference between the results obtained by means of TOMLAB and MATLAB my be explained by the properties of the optimisation criterion defined by Eq.(8). In Fig. 3, Fig. 4 and Fig. 5, selected cross-sections of this criterion show its multiple minima. Those cross-sections have been obtained for the noise-free data using the following formula for defining the variability of the parameters:

$$\tilde{a}_\nu = \dot{a}_\nu + s \cdot \Delta a_\nu \text{ for } \nu = 0, 1, 2 \tag{12}$$

$$\tilde{b}_\nu = \dot{b}_\nu + s \cdot \Delta b_\nu \text{ for } \nu = 0, \pm 1, \pm 2, \pm 3 \tag{13}$$

where $\dot{a}_\nu$ and $\dot{b}_\nu$ are the values of the parameters obtained by means of TOMLAB, and $s \in [-1, 1]$ is parameter characterising the relative detuning from those values.

Table 1. Summary of numerical experiments

σ_η	Parameter or indicator		
	Symbol	**TOMLAB value**	**MATLAB value**
0	a_0	-0.212	-0.212
	a_1	0.924	0.923
	a_2	-1.499	-1.499
	b_{-3}	1743.2	1716.7
	b_{-2}	-4096.2	-4014.9
	b_{-1}	575.2	487.9
	b_0	3572.7	3635.9
	b_1	575.3	489.0
	b_2	-4096.1	-4010.9
	b_3	1743.2	1713.5
	J	$9.67\cdot10^{-5}$	$8.30\cdot10^{-3}$
	$\Delta_2\left[\hat{\mathbf{x}}^{cal}\right]$	$8.20\cdot10^{-6}$	$5.35\cdot10^{-4}$
	$\Delta_\infty\left[\hat{\mathbf{x}}^{cal}\right]$	$3.18\cdot10^{-5}$	$2.11\cdot10^{-3}$
	$\Delta_2\left[\hat{\mathbf{x}}^{val}\right]$	$7.14\cdot10^{-5}$	$5.93\cdot10^{-4}$
	$\Delta_\infty\left[\hat{\mathbf{x}}^{val}\right]$	$2.39\cdot10^{-5}$	$2.87\cdot10^{-3}$
10^{-4}	a_0	-0.209	-0.039
	a_1	0.917	0.352
	a_2	-1.494	-1.051
	b_{-3}	1743.2	1788.9
	b_{-2}	-4096.2	-3918.8
	b_{-1}	575.6	585.1
	b_0	3572.7	3740.8
	b_1	576.4	605.1
	b_2	-4096.1	-3876.3
	b_3	1743.2	1856.5
	J	$3.27\cdot10^{-1}$	2.04
	$\Delta_2\left[\hat{\mathbf{x}}^{cal}\right]$	$2.04\cdot10^{-2}$	$1.61\cdot10^{-1}$
	$\Delta_\infty\left[\hat{\mathbf{x}}^{cal}\right]$	$5.04\cdot10^{-2}$	$6.24\cdot10^{-1}$
	$\Delta_2\left[\hat{\mathbf{x}}^{val}\right]$	$2.25\cdot10^{-2}$	$1.56\cdot10^{-1}$
	$\Delta_\infty\left[\hat{\mathbf{x}}^{val}\right]$	$7.52\cdot10^{-2}$	$6.23\cdot10^{-1}$
10^{-3}	a_0	-0.181	-0.797
	a_1	0.794	1.771
	a_2	-1.404	-1.296
	b_{-3}	-67.00	2614.8
	b_{-2}	-61.29	-2048.1
	b_{-1}	67.26	862.9
	b_0	140.59	5359.1
	b_1	67.26	862.9
	b_2	-61.41	-2048.1
	b_3	-67.20	2614.7
	J	$3.90\cdot10^{-1}$	3.32
	$\Delta_2\left[\hat{\mathbf{x}}^{cal}\right]$	$3.16\cdot10^{-2}$	$2.91\cdot10^{-1}$
	$\Delta_\infty\left[\hat{\mathbf{x}}^{cal}\right]$	$1.20\cdot10^{-1}$	$7.97\cdot10^{-1}$
	$\Delta_2\left[\hat{\mathbf{x}}^{val}\right]$	$2.91\cdot10^{-2}$	$2.67\cdot10^{-1}$
	$\Delta_\infty\left[\hat{\mathbf{x}}^{val}\right]$	$1.22\cdot10^{-1}$	$6.79\cdot10^{-1}$

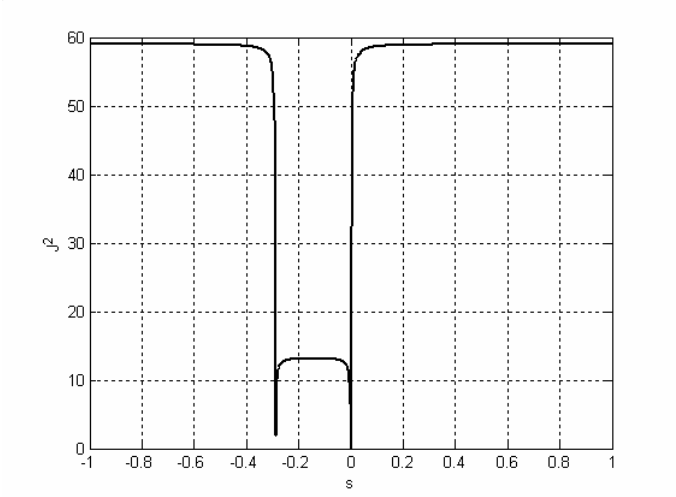

Fig. 3. The cross-section of the squared criterion J, corresponding to $\Delta a_0 = 60$ and $\Delta b_0 = 60$ (other parameters fixed).

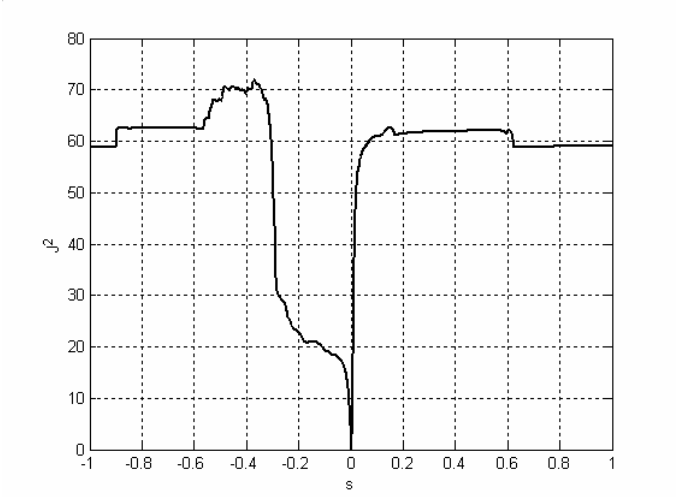

Fig. 4. The cross-section of the squared criterion J, corresponding to $\Delta a_1 = 60$ and $\Delta b_0 = 60$ (other parameters fixed).

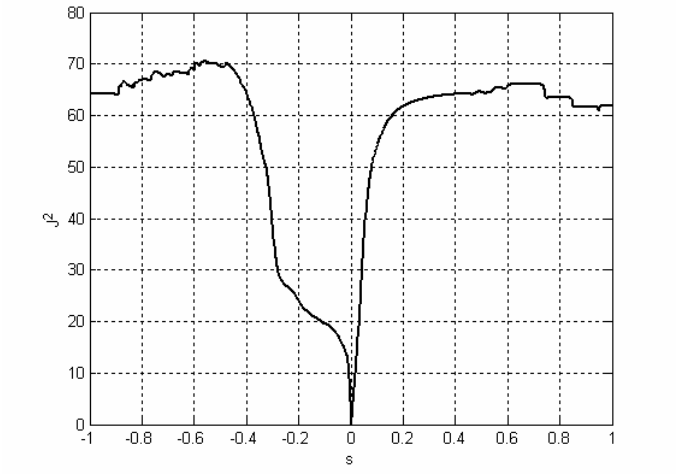

Fig. 5. The cross-section of the squared criterion J, corresponding to $\Delta a_2 = 60$ and $\Delta b_0 = 60$ (other parameters fixed).

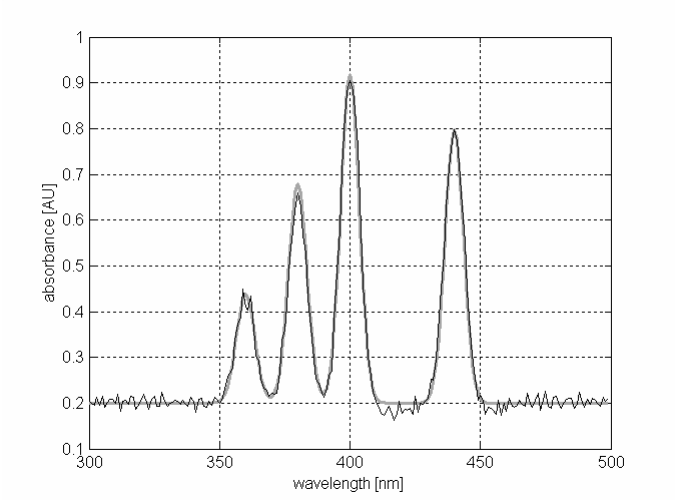

Fig. 6. The result of reconstruction, obtained for the validation data using the estimates of the reconstruction parameters provided by TOMLAB (thin black line) compared with the reference spectrum (bolder lighter line).

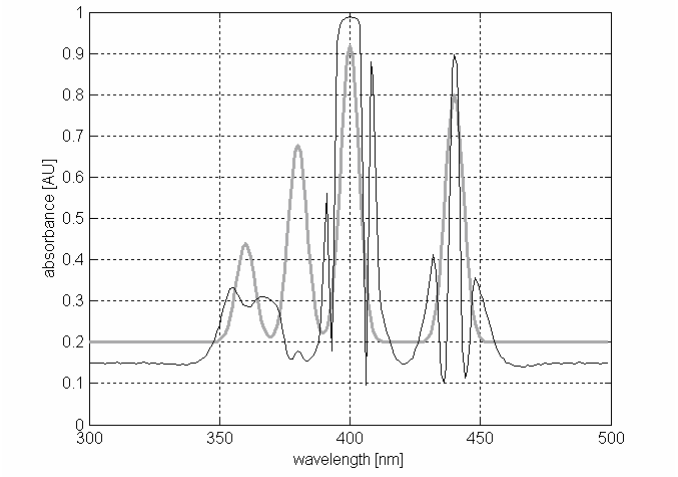

Fig. 6. The result of reconstruction, obtained for the validation data using the estimates of the reconstruction parameters provided by MATLAB (thin black line) compared with the reference spectrum (bolder lighter line).

4. CONCLUSION

A new inverse-model-based method for spectrum reconstruction has been proposed and studied using a TOMLAB procedure of global optimization and a MATLAB procedure of local optimization. It has been demonstrated that the use of global optimization for spectrophotometer calibration provides a significant reduction of the contents of artefacts, as well as of the measurement uncertainties expressed in terms of the indicators defined by Eq.(11). This difference is illustrated in Fig. 5 and Fig. 6 where the same spectrum from Fig. 2 has been reconstructed using the results of calibration obtained by means of TOMLAB and MATLAB.

ACKNOWLEDGMENTS

This work is supported by the State Committee of Scientific Research, Poland (grant # 4 T10C 017 24).

REFERENCES

[1] Analytical Spectral Devices, Inc.: "Using NIR Technology for Determining Product Quality of Industrial Plastics", "Determining the Composition of Carpet Fiber", "Real-Time Monitoring of the Polymerization Process by NIR Transmittance", "Quantitative Analysis of Concrete Samples Via NIR", "Quantification of Various Fatty Acids in Whole Canola Seed Using NIR Technology", "NIR Analysis of Rice Samples for Free Fatty Acid and Moisture", "Using NIR Reflectance to Analyze Menthol Concentration in Tobacco", "Using NIR Reflectance to Analyze Protein Content in Gluten Products"; Application Notes, *http://www.asdi.com/publications-applications.asp*

[2] D. Bakhmutov, S. Gonchukov, O. Kharchenko, O. Nikiforova, and Yu. Vdovin: "Early dental caries detection by fluorescence spectroscopy", *Laser Phys. Lett*., Vol. l, No. 11, 2004, pp. 565-569.

[3] D. Bradley: "Extra virgin or fake?, *spectroscopyNOW*.com, August 5, 2004, *http://www.spectroscopynow.com*

[4] E. Ergun, B. Demirata, G. Gumus, and R. Apak: "Simultaneous determination of chlorophyll a and chlorophyll b by derivative spectrophotometry", *Anal. & Bioanal. Chem.*, Vol. 379, No. 5-6, July 2004, pp. 803–811.

[5] I. Esteban-Diez, J. M. Gonzalez, and C. Pizarro: "Prediction of sensory properties of espresso from roasted coffee samples by near-infrared spectroscopy", *Analytica Chimica Acta*, Vol. 525, 2004, pp. 171-182.

[6] J. Ghasemi, N. Shahabadi, and H. R. Seraji: "Spectrophotometric system and method for the identification and simultaneous determination of cobalt, copper and nickel using nitroso-R-saltin alloys by partial least squares", *Analytica Chimica Acta*, Vol. 510, No. 1, May 2004, pp. 121-126.

[7] Haiyan Song, and Yong He:"Evaluating Soil Organic Matter with Visible Spectroscopy", *Proc. Instrum. & Meas. Technol. Conf. – IMTC/2005 (Ottawa, Canada, May 17-19, 2005)*, pp. 1321-1324.

[8] I. Hiroaki, N. Toyonori, and T. Eiji: "Measurement of pesticide residues in food based on diffuse reflectance IR spectroscopy", *IEEE Trans. Instrum. & Meas.*, Vol. 51, No. 5, October 2002, pp. 886-890.

[9] P. Hourant, V. Baeten, M. T. Morales, M. Meurens, and R. Aparicio: "Oil and Fat Classification by Selected Bands of Near-Infrared Spectroscopy", *Applied Spectroscopy*, Vol. 54, No. 8, 2000, pp. 1168-1174.

[10] K. S. Johnson, and L. J. Coletti: "*In situ* ultraviolet spectrophotometry for high resolution and long-term monitoring of nitrate, bromide and bisulfide in the ocean", *Deep-Sea Research I*, Vol. 49, 2002, pp. 1291–1305.

[11] S. E. Kays, Douglas D. A., and Miryeong Sohn: "Prediction of fat in intact cereal food products using near-infrared reflectance spectroscopy", *J. Sci. Food Agric.,* Vol. 85, 2005, pp. 1596–1602

[12] Tenhunen J., H. Kopola, and R. Myllylä: "Non-Invasive Glucose Measurement Based on Selective Near-Infrared Absorption; Requirements on Instrumentation and Spectral Range", *Measurement – J. IMEKO*, Vol. 24, 1998, pp. 173-177.

[13] Thermo Electron Corp.: "A Bibliography of UV-Visible Spectrophotometric Analyses of Wines and Musts", *http://www.thermo.com/eThermo/CMA/PDFs/Various/File_24917. pdf.*

[14] P. A. Jansson (ed.), *Deconvolution of Spectra and Images*, Academic Press Inc., New York, 1997.

[15] F. Cuesta Sánchez, S. C. Rutan, M. D. Gil García, and D. L. Massart, "Resolution of Multicomponent Overlapped Peaks by the Orthogonal Projection Approach, Evolving Factor Analysis and Window Factor Analysis", *Chemeometrics & Intelligent Lab. Systems*, Vol. 36, 1997, pp. 153-164.

[16] D. K. Buslov, and N. A. Nikonenko, "*A Priori* Estimation of the Parameters of the Method of Spectral Curve Deconvolution", *Appl. Spectroscopy*, Vol. 52, No. 4, 1998, pp. 613-620.

[17] R. Salvetat, P. Eullaffroy, and R. Popovic, "Analyse de spectres complexes mesurés par un spectromètre à reseau: déconvolution, méthose d'entropie maximale et prédiction linéaire", *Canadian J. Anal. Sci. & Spectroscopy*, Vol. 42, No. 6, 1997, pp. 177-184.

[18] M. S. Ramsey, and P. R. Christensen, "Mineral Abundance Determination: Quantitative Deconvolution of Thermal Emission Spectra", *J. Geophysical Res.*, Vol. 103, No. B1, January 1998, pp. 577-596.

[19] A. R. Pratt, N. S. McIntyre, and S. J. Splinter: "Deconvolution of Pyritre, Marcasite and Arsenopyrite XPS Spectra Using the Maximum Entropy Method", *Surface Science,* Vol. 396, 1998, pp. 266-272.

[20] M. Ben Slima, L. Szczeciński, D. Massicotte, R. Z. Morawski, and A. Barwicz, "Algorithmic Specification of a Specialized Processor for Spectrometric Applications", *Proc. IEEE Instrum. & Meas. Technol. Conf. – IMTC'97 (Ottawa, Canada, May 19-21, 1997)*, pp. 90-95.

[21] L. Szczecinski, R. Z. Morawski, and A. Barwicz: "Numerical Correction of Spectrometric Data Using a Rational Filter", *J. Chemometrics,* Vol. 12, issue 6, 1998, pp. 379 - 395.

[22] R. Z. Morawski, A. Miękina, and A. Barwicz: "Combined Use of Tikhonov Deconvolution and Curve Fitting for Spectrogram Interpretation", *Instrum. Science & Technology*, Vol. 24, No. 3, 1996, pp. 155-167.

[23] R. Z. Morawski, A. Miękina, and A. Barwicz: "The Use of Deconvolution and Iterative Optimisation for Spectrogram Interpretation", *IEEE Trans. Instrum. & Meas.*, Vol. 46, No. 4, August 1997, pp. 1049-1053.

[24] P. Sprzęczak, and R. Z. Morawski: "Cauchy Filters versus Neural Networks when Applied for Reconstruction of Absorption Spectra", *IEEE Trans. Instrum. & Meas.*, Vol. 51, No. 4, August 2002, pp. 815-818.

[25] M. P. Wiśniewski, R. Z. Morawski, and A. Barwicz: "An Adaptive Rational Filter for Interpretation of Spectrometric Data", *IEEE Trans. Instrum. & Meas.*, Vol. 52, No. 3, June 2003, pp. 966-972.